Report on 3,143.6-km Time and Frequency Transfer Fiber Link with Ps-level Stability

Bo Liu[1,2,3†], Xinxing Guo[1,2,3†], Jiang Chen[1,2,3], Yanli Zhou[4*], Tao Liu[1,2,3*], Ruifang Dong[1,2,3*], and Shougang Zhang[1,2,3]

[1]*National Time Service Center, Chinese Academy of Sciences, Xi'an 710600, China*
[2]*University of Chinese Academy of Sciences, Beijing 100039, China*
[3]*Key Laboratory of Time Reference and Applications, Chinese Academy of Sciences, Xi'an 710600, China*
[4]*China Mobile Communications Group Shaanxi Co., Ltd, Xi'an 710600, China*

(Received 18 October 2024; accepted manuscript online 25 December 2024)

This letter describes the implementation of a high-precision time and frequency transmission system using a two-way and wavelength division multiplexing scheme over 3,143.6 km of field fiber links, connecting 21 sites between Xi'an and Beijing, China. This scheme incorporates a link noise clean-up system (LNCUS), wherein a controlled very-low-phase noise BVA oscillator acts as an internal frequency source at the relay site to effectively suppress the interference caused by the fiber link noise. Additionally, the high-stability pulse generation technology in the LNCPS provides sufficient short-term stability to significantly improve the stability of the fiber time transfer. The results indicate a time transfer stability in terms of time deviation (TDEV) of less than 2.07 ps@1s, 5.9 ps@100,000s, and combined uncertainty of less than 49.29 ps for the 3,143.6 km field fiber link. The results represent a significant breakthrough in achieving high-accuracy time transfer and continuous operation over ultralong-span field optical fibers exceeding 3,000 km for the first time. This enabled time transfer and synchronization services over the longest international optical fiber distance, thereby establishing a fundamental basis for constructing a nationwide high-precision time service through optical fiber networks.

DOI: 10.1088/0256-307X/42/1/014202 CSTR: 32039.14.0256-307X.42.1.014202

There is an urgent demand for sub-nanosecond or even picosecond high-precision time and frequency transmissions in the domains of fundamental scientific research, advanced engineering applications, national defense science and technology, and other related fields. Consequently, the establishment of a high-precision time and frequency transfer system with enhanced transfer performance is an important concern.[1–6] The process of traditional time and frequency transfer solutions typically leads to significant degradation in the accuracy of high-performance clock sources, and thus they are inadequate to meet requirements of long-distance high-precision time applications.[7–11] With the rapid development of laser technology and fiber optic communication, time transmission over fiber (TTOF) utilizes the consistency of the bidirectional path of the fiber optic link and the stability of the channel. Its time transfer accuracy can reach picoseconds, which currently corresponds to the best application prospect with the highest accuracy of time transmission.[12–15] Fiber optic time-transfer technology has witnessed rapid development in recent years, leading to significant enhancements in the distance, accuracy, and stability of time transfer. AGH University in Poland conducted an experiment in 2016, wherein they transmitted a time signal over a distance of 615 km using fiber optics and time calibration with an accuracy well below 50 ps.[16] The LPL utilized the White Rabbit Precision Time Protocol (WR-PTP) to propagate time and frequency over a 500 km fiber optic link in 2022, achieving latency fluctuations of 400 ps at 125 km and 2.5 ns at 500 km.[17] In 2021, a team from Shanghai Jiaotong University used BTDM-SFSW for time transfer in a 13,134 km laboratory disk fiber (re-circulating the time signals 33 laps in the 398 km fiber loop), time synchronization stability in terms of a TDEV of less than 32 ps@10s, and a combined uncertainty of less than 89.6 ps.[18]

In 2021, China will comprehensively implement the construction of the "High Accuracy Ground-based Time Service System" project, aiming to establish a high-precision fiber time synchronization network with a deviation from the national standard time signal exceeding 100 ps and achieving nationwide coverage of high-precision fiber time transmission over a distance greater than 20,000 kilometers. The authors successfully validated the performance metrics of long-haul fiber optic time transfer multiple times in laboratory and field fiber links. A typical example is the reported TTOF in 1,839 km of field fiber links in 2023, exhibiting a time transmission stability of 6.5 ps@1s and 4.6 ps@40000s.[19] Recently, we successfully accomplished time transmission on the 3143.6 km Xi'an Beijing field fiber loop link, achieving time transfer stability with a TDEV of less than 2.07 ps@1s and

†These authors contributed equally to this work.
*Corresponding author. Email: zhouyanli@sn.chinamobile.com; taoliu@ntsc.ac.cn; dongruifang@ntsc.ac.cn
© 2025 Chinese Physical Society and IOP Publishing Ltd. All rights, including for text and data mining, AI training, and similar technologies, are reserved.

5.9 ps@100,000s and a combined uncertainty of less than 49.29 ps. The simultaneous transmission of the 10 MHz frequency signal also demonstrated exceptional stability levels, reaching 5.7×10^{-13}@1s and 4.3×10^{-16}@100,000s. These results are pioneering in high-precision field fiber time transmission spanning over 3,000 km, thereby establishing a solid groundwork for delivering top-notch time services to users across China's extensive fiber network.

The output power of the time transmitter laser is 0 dBm, and the acceptable optical attenuation of the receiver photodetector is −25 dB. To compensate for the optical loss of 0.3–0.35 dB/km caused by the fiber optic link, relay/download devices are usually arranged at intervals of 40–70 km in the long-distance fiber optic time transfer link. Therefore, field fiber links and relay sites of China Mobile Communications Group Co., Ltd. were utilized to equip 42 pieces of equipment (1 time transmitter, 1 time receiver, and 40 relay/download devices) in the 3,143.6 km (21 sites) field fiber loop link between Chang'an campus of the National Time Service Center in Xi'an and Beijing Mentougou sites spanning four provinces as follows: Shaanxi, Shanxi, Hebei, and Beijing, as depicted in Fig. 1. The time transmitter is installed at the Chang'an campus (local station) in Shaanxi Province, and it traverses through 3 relay stations in Shaanxi (Weinan, Pucheng, Heyang), 10 relay stations in Shanxi (Hejin, Houma, Linfen, Huozhou, Jiexiu, Qixian, Yuji, Taiyuan, Nanjiang, Taiyang), 5 relay stations in Hebei (Kulongfeng, Shijiazhuang, Dingzhou, Baoding, Dingxing), and 2 relay stations in Beijing (Liangxiang, Mentougou). Finally, it returns to the Chang'an campus (remote station) with another fiber in the same relay sites. In order to facilitate the verification of the results obtained from time transfer experiments, the time receiver was also installed at the Chang'an campus. The 20 relay sites were each equipped with two relay/download devices to amplify optical signals and fulfill the high-precision time-signal requirements of the sites. The fiber distances between adjacent sites are shown in Fig. 1. The longest section of the relay link was observed at the Weinan-Pucheng sites, spanning a total distance of 96 km with a loss of 25.12 dB.

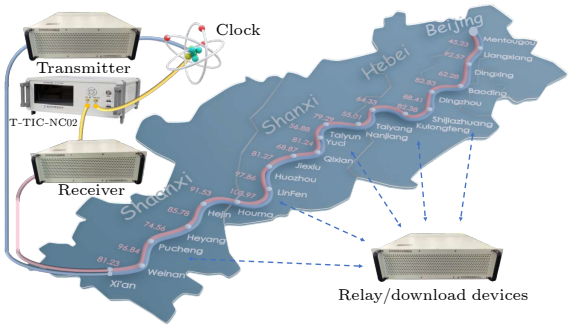

Fig. 1. Geographical distribution of the 3143.6-km field fiber link.

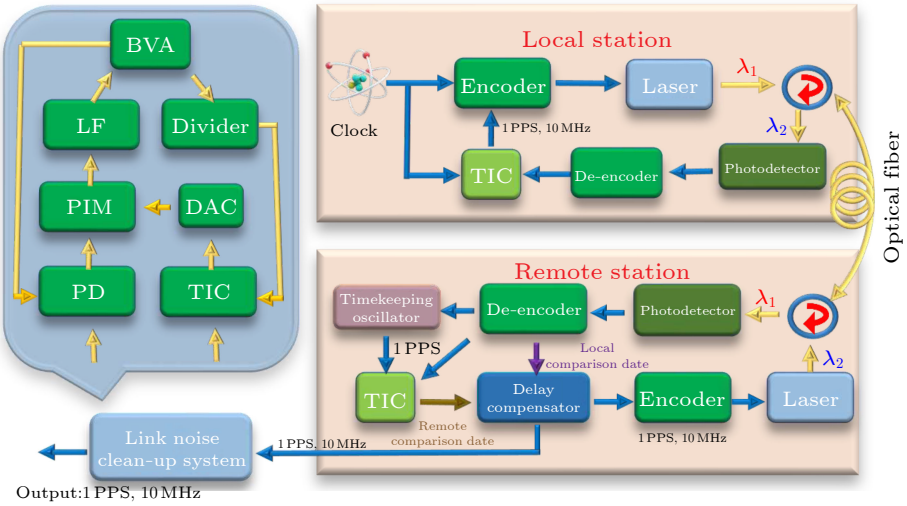

Fig. 2. Simplified block diagram of the time transfer system.

The principle of two-way fiber time transmission based on wavelength division multiplexing (WDM) is illustrated in Fig. 2. The time transfer scheme is analogous to our previous approach employed in earlier fiber time transfer experiments, as documented in Refs. [12,13,19]. The key distinction lies in the implementation of a link noise cleanup system (LNCUS), which is incorporated not only at remote stations and at relay sites. In a local station, the time signal (1 pulse per second, 1 PPS) and local comparison data are encoded at a frequency of 10 MHz and modulated onto an optical carrier with a wavelength of λ_1 (1,548.5 nm). The optical signal passes through an optical circulator and a fiber link to reach the remote station. At the remote station, optical signals from the local station are separated using an optical circulator, converted into electrical signals by a photodetector, and then decoded to output the 1 PPS and comparison data from the local station. For the relay/download device, the optical signal from the previous site is divided into two paths after passing through an optical beam splitter, one of which is transmitted to the next site using an O-E-O scheme,[12] and the other path outputs the transferred T/F signals to the relay

user in 1 PPS and 10 MHz frequency after being corrected for the fiber transfer delays via module combinations of photodetector, TIC, processor, and T/F signal recovery. Thus, as shown in Fig. 1, there are 40 relay/download devices which are required to perform relay as well as download functions at each site.[19] The reference source at the remote station generates three outputs from its delayed compensator: one is compared with the decoded 1 PPS to obtain remote comparison data; another is encoded and modulated onto a laser carrier with a wavelength of λ_2 (1,549.3 nm) for transmission to the local station; and the third serves as the output for the 1 PPS from the remote station. Based on local and remote comparison data, precise synchronization between the outputted 1 PPS from the remote station and inputted 1 PPS to the local station is achieved via control of the time delay compensator by the time receiver in the remote station.

Following the extension of fiber distance and the proliferation of relay sites, the 1 PPS is susceptible to external factors such as fluctuations in environmental temperature, electromagnetic interference, and random vibrations when transmitted over long distances via the fiber. The phase noise and short-term stability indicators of the 1 PPS experienced significant deterioration. Moreover, given the inherent delay control lag associated with long-distance fiber transmission, it is impractical to effectively manage real-time fast-delay jitter while substantially reducing the ability to suppress rapid noise. Consequently, noise in the fiber link emerges as a primary factor affecting short-term stability during fiber time transmission.[20]

An LNCUS was proposed in the 3,143.6 km fiber time transfer system as shown on the left side of Fig. 2. The LNCUS included an extremely low-phase-noise BVA oscillator as an internal frequency source. This improves the short-term stability of the output frequency signal, which can be stabilized on the order of 1×10^{-13}@1s. The phase detection of the 10 MHz signal output from the remote station and the 10 MHz generated by the BVA oscillator in the LNCUS is achieved via dual-frequency mixing measurement technology (setting the frequency difference to 100 Hz increases measurement resolution by five orders of magnitude). The DAC was then controlled by the phase measurement value to lock and stabilize the BVA oscillator. The loop bandwidth of the LNCUS ranged from approximately 30 to 50 s (25 mHz). In the configuration, high-stability pulse generation technology was utilized for the low-noise 10 MHz output of the BVA oscillator, which was divided into a low-noise 1 PPS time signal. The time-difference measurement module implements a precise measurement of the time difference between the low-noise 1 PPS time signal and remote output 1 PPS. The measured time difference was processed using an arithmetic processing unit to eliminate the effect of noise and calculate necessary control parameters. Based on the calculated control parameters, delay controller adjustments are made by the arithmetic processing unit to synchronize with the reference time signals, and this effectively suppressed delay drift and providing users or subsequent stations with highly stable, low-noise 1 PPS and 10 MHz signals.

To visualize the performance results of the 3,143.6 km field fiber time transfer, the transfer system measured the time difference between the input 1 PPS of the time transmitter and output 1 PPS of the time receiver based on a common time and frequency reference clock (active hydrogen clock vch-1003m). The measurements were conducted using T-TRIC-NC02 commercial time-interval counters (RMS resolution better than 1 ps) from TIME-TRANSFER. Figure 3 shows the measured results for 3,143.6 km fiber time transfer measurement data for approximately two weeks, over 1,200,000 s. The time difference measured by the LNCUS exhibits a peak-to-peak value (3σ) of 151 ps with a standard deviation (SD) of 18.9 ps. This exceeds that of the non-LNCUS measurement on the same fiber, which displays a peak-to-peak value (3σ) of 265 ps and a standard deviation (SD) of 24.1 ps.

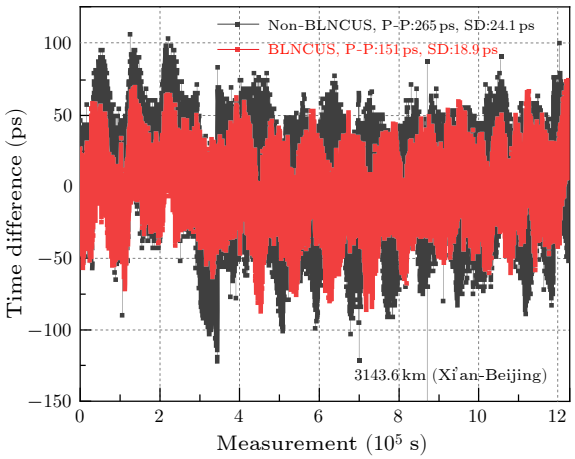

Fig. 3. Time difference of the 3143.6-km field fiber link over two weeks.

TDEV quantifies the deviation of time-transfer measurements from a known reference time over a specified averaging period. It essentially evaluates the extent to which the time-transfer signal fluctuates around an average over time. As shown in Fig. 4, the use of the LNCUS demonstrates a significant enhancement in short-term stability with a reduction from 11.5 ps@s to 2.07 ps@s and from 6.2 ps@10s to 1.7 ps@10s. Given that the loop bandwidth of the LNCUS ranges between approximately 30 and 50 s (25 mHz), it does not achieve an index of −14 magnitude order for the BVA oscillator at 100 s, and this results in an introduced deterioration of time stability by 4.8 ps@100 s. Long-term stability in fiber optic time transfer systems is affected by a combination of thermal expansion and contraction, temperature-induced dispersion, laser linewidth and frequency stability, and digital processing factors. These factors can cause drift or degradation over time and cause inaccuracies in the time synchronization. Given the significant temperature control cavity and precise loop servo-locking accuracy, long-term stability does not significantly deteriorate and is measured at approximately 5.9 ps@10,000 s and 4.9 ps@200,000, and the results align with the transfer metrics obtained for the non-LNCUS.

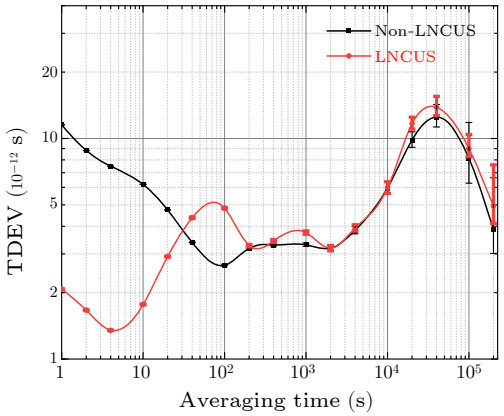

Fig. 4. Measured time transfer stability in terms of time deviation (TDEV) over the 3143.6 km fiber link.

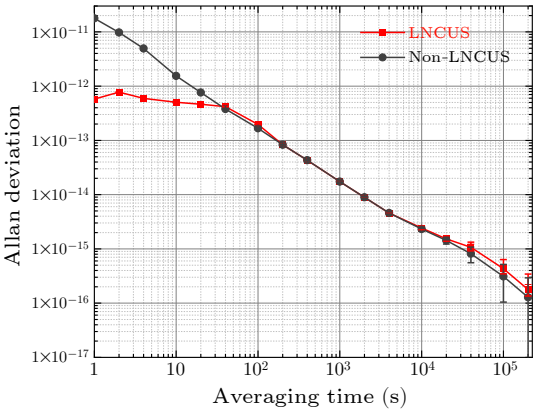

Fig. 5. ADEV for 10 MHz frequency transfers over the 3143.6 km fiber loop link.

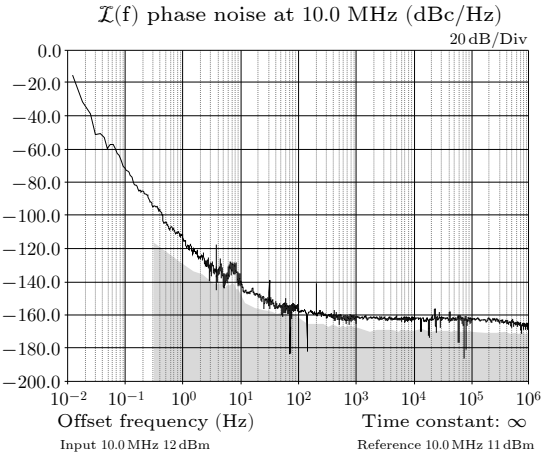

Fig. 6. Measured phase noise spectra of fiber frequency transfer at the 3143.6 km fiber loop link.

The frequency transfer capability of the system was then examined. The phase noise analyzer (Symmetricom, TSC-5120A) was triggered by the same 10-MHz signal that was input into the local reference clocks, and the second channel was connected to the frequency output of the time receiver transmitted through a 3,143.6 km fiber loop link to observe the phase fluctuations. The LNCUS of the ADEV as calculated from a two-weeks measurement is shown in Fig. 5, demonstrating an achieved frequency stability of 5.7×10^{-13}@s and 4.3×10^{-16}@100,000 s. The 10 MHz frequency data from Non-LNCUS is shown in Fig. 5 for comparison purposes, and the ADEV is 1.8×10^{-11}@s and 3.1×10^{-16}@100,000 s. Furthermore, Fig. 6 shows the phase noise at 10 MHz for the LNCUS when continuously tracking the reference clocks. The measurements correspond to −109.2 dBc/Hz@1 Hz, −154.2 dBc/Hz@100 Hz, and −162.2 dBc/Hz@100 kHz.

Table 1. Uncertainty budget for the 3,143.6-km field fiber link.

Uncertainty source	Uncertainty contribution (ps)	Uncertainty type
$u_{\mathrm{ref-out}}$	18.9	A
u_{tic}	7.07	B
u_{h}	9.6	A
u_{tc}	1.8	A
$u_{\lambda-\mathrm{D}}$	41.96	A&B
u_{pmd}	1.12	B
u_{sagnac}	12.88	B
Combined uncertainty	49.29	

Fiber time transfer uncertainty refers to the limitations and errors that can occur when synchronizing the time between two locations using fiber optic cables. This synchronization is essential for applications in telecommunications, navigation systems, and scientific research that require precise timekeeping. The uncertainty budget for the proposed time transfer system over the equivalent 3,143.6 km field fiber link is presented in Table 1. In this context, type A uncertainty is assessed through a statistical analysis of a series of experimental measurements, whereas type B uncertainty encompasses data obtained from nonexperimental sources such as data sheets, calibration reports, and journal articles. The last line of the table contains the standard combined uncertainty of the time transfer represented by u_{c}. The standard combined uncertainty refers to the total uncertainty in a measurement arising from multiple sources. It is calculated by combining various individual uncertainties that contribute to the overall uncertainty of the measured values. Row 1 in Table 1 lists the uncertainty components related to the measurement of time intervals in the evaluation reference clocks to the remote station time receiver, $u_{\mathrm{ref-out}}$. The uncertainty was assessed at 18.9 ps based on measurements obtained over a two-week time interval, as shown in Fig. 3. The second term represents the uncertainty u_{tic} generated by TICs in the two-way transfer process at A and B. This value is associated with factors such as the measured time interval, reference clock frequency stability, cable and connector additive jitter errors, input-signal trigger level, and time-interval measurement noise. Based on extant studies,[19] this uncertainty was quantified as 7.07 ps. The third term represents the uncertainty of the time-transfer hardware device, u_{h}. This introduces time errors due to temperature effects including variations in electronic components such as the phase identification module and phase-locked loop (PLL). Optical devices, such as optocouplers and optical switches, also contribute to propagation errors.[12] Overall, this item exhibited an uncer-

tainty of 9.6 ps. The fourth term indicates uncertainty $u_{\rm tc}$ caused by the delay compensation accuracy. In the study, we use a Field Programmable Gate Array (FPGA) whole-cycle shifted combined with a PLL precision phase-shifted ground remote station multilevel delay compensation technique. When comparison to extant studies,[12] the uncertainty of this term is 1.8 ps. The uncertainty in fiber optic time transfer due to fiber dispersion coupled with wavelength differences of bidirectional lasers can lead to significant timing errors, especially over long distances. The fifth term is uncertainty $u_{\lambda-\rm D}$ due to the fiber dispersion factor coupled to the wavelength difference of the bidirectional laser. The uncertainty of the difference in wavelengths is due to inconsistent initial SFP laser calibration and instability of SFP laser emitters caused by E/O converters in relay/download devices.[19,21] The contribution to total uncertainty is calculated for $D = 17\,\text{ps/km·nm}$. The dominant contribution of this term indicates the implementation of dispersion compensation or reduction techniques to minimize the sensitivity coefficient, which is desirable. The uncertainty associated with chromatic dispersion is due to potential measurement inaccuracies and a slight dependence on fiber temperature, typically ranging from -3 to $1\,\text{fs/(nm·km·K)}$ for various types of fibers.[21] The provided value was based on an analysis of the vendor-declared performance of optical spectrum analyzers and our experience with laser transmitter designs. This contribution is calculated given a wavelength difference of 0.8 nm and corresponds to 41.96 ps. In future studies, fiber dispersion compensation and bidirectional laser wavelength matching strategies can be used to minimize uncertainty caused by these effects. The sixth term is the uncertainty $u_{\rm pmd}$ due to PMD dispersion. PMD occurs when different polarization modes of light travel at different speeds through an optical fiber, and this leads to the spread of optical pulses over time. The PMD is typically quantified in terms of the PMD coefficient, which is expressed in picoseconds per square root kilometer ($\text{ps}/\sqrt{\text{km}}$). This coefficient determines the extent of delay variation expected over a certain distance. In the G.652 fibers, the PMD coefficient was typically lower than $0.05\,\text{ps}/\sqrt{\text{km}}$. In the last item, the link asymmetry induced by the Sagnac effect is non-negligible when a rotating reference coordinate system (e.g., a geocentric reference coordinate system) is considered and when the source and target of the signal exhibit different longitudes. Based on Ref. [22], the uncertainty $u_{\rm sagnac}$ introduced by the Sagnac effect correction was estimated to be 12.88 ps.

$$u_{\rm c} = \sqrt{u_{\rm ref-out}^2 + u_{\rm tic}^2 + u_{\rm h}^2 + u_{\rm tc}^2 + u_{\lambda-\rm D}^2 + u_{\rm pmd}^2 + u_{\rm sagnac}^2}. \tag{1}$$

Overall, the combined uncertainty $u_{\rm c}$ of the time transfer system over 3143.6 km of fiber was estimated to be 49.29 ps.

In summary, we report that the Xi'an-Beijing section of the "High Accuracy Ground-based Time Service System" project achieved ps-level stability time transfer over a record distance of 3,143.6 km. The system uses LNCUS to suppress fiber link noise, and the TDEV of 1 PPS exceeded 2.07 ps@1s, 5.9 ps@100,000 s, with a combined uncertainty assessment of 49.29 ps. The ADEV of the 10 MHz frequency exceeded 5.7×10^{-13}@1s and 4.3×10^{-16}@100,000 s. The study provides important support for the construction of modern high-precision time and frequency systems in China.

References

[1] Li J, Liu Y, Zhao W, Zhu T, Wang Y, and Hu K 2024 *Sci. Rep.* **14** 19150

[2] Nehbit P K, Glaser S, Sakic P, Balidakis K, Heinkelmann R, Schuh H, and Konak H 2023 *Adv. Space. Res.* **72** 3037

[3] van Bemmel I M, Kettenis M, Small D, Janssen M, Moellenbrock G A A, Petry D, Goddi C, Linford J D D, Rygl K L J, Liuzzo E, Marcote B, Bayandina O S S, Schweighart N, Verkouter M, Keimpema A, Szomoru A, and van Langevelde H J 2022 *Publ. Astron. Soc. Pac.* **134** 114502

[4] Du B and Li W 2024 *Analog Integr. Circ. Sig. Process* **118** 147

[5] Wang K and Feng C J 2024 *Phys. Lett. B* **855** 138875

[6] Pilipenko S V, Litvinov D A, Zakhvatkin M V, and Filetkin A I 2024 *Astron. Rep.* **68** 300

[7] Parker T E, Zhang V, Petit G, Yao J, Brown R C, and Hanssen J L 2022 *Metrologia* **59** 035007

[8] Lima M V and Tarelho L V 2022 *IEEE Latin-American Cference on Communications* (LATINCOM)

[9] Zeng T, Shen Q, Cao Y, Guan J Y, Lian M Z, Han J J, Hou L, Lu J, Peng X X, Li M, Liu W Y, Wu J C, Wang Y, Yin J, Ren J G, Jiang H F, Zhang Q, Peng C Z, and Pan J W 2024 *Photonics Res.* **12** 1274

[10] Zhang X, Hu L, Deng X, Zang Q, Liu J, Jiao D, Gao J, Dong R, Liu T, Wu G, Chen J, and Zhang S 2022 *IEEE Photonic Tech. L* **34** 413

[11] Lima M V and Tarelho L V 2022 LATINCOM.

[12] Liu B, Guo X, Kong W, Liu T, Dong R, and Zhang S 2022 *Nat. Photonics.* **9** 522

[13] Guo X, Qiu Y, Liu B, Kong W, Liu T, Dong R, and Zhang S 2022 *Appl. Sci.* **12** 6643

[14] Amemiya M, Imae M, Fujii Y, Suzuyama T, Hong F L, and Takamoto M 2010 *IEEE Transactions on Instrumentation and Measurement* **59** 631

[15] Krehlik P, Sliwczynski L, and Buczek L 2021 *IEEE Transactions on Ultrasonics, Ferroelectrics, and Frequency Control* **68** 899

[16] Krehlik P, Sliwczynski L, Buczek L, Kolodziej J, and Lipinski M 2016 *IEEE Transactions on Ultrasonics, Ferroelectrics, and Frequency Control* **63** 993

[17] Kaur N, Frank F, Pinto J, Tuckey P, and Pottie P E 2022 *IEEE Transactions on Ultrasonics, Ferroelectrics, and Frequency Control* **69** 892

[18] Zuo F, Xie K, Hu L, Chen J, and Wu G 2021 *J Lightwave Technol.* **39** 6373

[19] Guo X X, Hou B, Liu B, Yang F, Kong W C, Liu T, Dong R F, and Zhang S G 2024 *Chin. Phys. Lett.* **41** 064202

[20] Sliwczynski Ł and Kolodziej J 2013 *IEEE Trans. Instrum. Meas.* **62** 253

[21] Krehlik P, Sliwczynski Ł, Buczek Ł, and Lipinski M 2012 *IEEE Transactions on Instrumentation and Measurement* **61** 2844

[22] Slapak M and Vojtech J 2018 *EFTF* p. 300